This is the accepted version of the article. To cite this article, please refer to the published version:
Guy Brammertz, Mohammad Shahjahan, Abdullah Bin Shams, Alex J. López García, Alejandro Pérez-Rodríguez, Jessica de Wild, Marc Meuris, Jef Poortmans, Bart Vermang. 2023. Fabrication and characterization of ZnS and ZnSe absorber layers for UV-selective transparent photovoltaics, Thin Solid Films 767:139671. https://doi.org/10.1016/j.tsf.2023.139671

Fabrication and characterization of ZnS and ZnSe absorber layers for UV-selective transparent photovoltaics.

Guy Brammertz[1,2,3], Mohammad Shahjahan[1,2,3], Abdullah Bin Shams[1,2,3], Alex J. López García[4], Alejandro Pérez-Rodríguez[4,5], Jessica de Wild[1,2,3], Marc Meuris[1,2,3], Jef Poortmans[1,2,3,6], Bart Vermang[1,2,3].

[1] Imec, imo-imomec, Thor Park 8320, 3600 Genk, Belgium.

[2] Hasselt University, imo-imomec, Martelarenlaan 42, 3500 Hasselt, Belgium

[3] EnergyVille, imo-imomec, Thor Park 8320, 3600 Genk, Belgium.

[4] Solar Energy Materials and Systems, Institut de Recerca en Energia de Catalunya (IREC), Jardins de les Dones de Negre, 1, 2ª pl, 08930, Sant Adrià del Besòs, Barcelona, Spain.

[5] IN2UB, Departament d'Enginyeria Electrònica i Biomèdica, Universitat de Barcelona, Carrer de Martí i Franquès 1, Barcelona, Spain.

[6] Department of Electrical Engineering, KU Leuven, Kasteelpark Arenberg 10, 3001 Heverlee, Belgium.

Abstract

We have fabricated ZnS, ZnSe and mixed Zn(S,Se) thin film layers for application as solar cell absorbers in ultraviolet (UV)-selective solar cells. We fabricated the thin film layers using a two-step process involving evaporation of the Zn layer followed by an anneal in an H_2S and/or H_2Se containing atmosphere. A study of the annealing conditions was performed to minimize hole formation in the thin film layer. A mixed Sulfur and Selenium containing layer was also developed in order to reach a 3 eV band gap, such that the layer absorbs all the UV light and leaves the visible light passing through. Next, we tried to increase the conductivity of the layer by adding extrinsic doping elements. Cu was found to increase the conductivity by more than three orders of magnitude, while leaving the transparency of the layer mostly unchanged. Finally, solar cell devices were fabricated using transparent back and front contacts and a NiO buffer layer. We could measure a very small photocurrent of about 100 $\mu A/cm^2$ and an open circuit voltage of about 500 mV under AM1.5G illumination.

Keywords

- Zinc selenide
- Zinc sulfide
- Zn(S,Se)
- Photovoltaics
- Solar cell
- Transparent photovoltaics

Highlights

- Fabrication of thin film Zinc selenide, Zinc sulfide and mixed Zinc sulfide-selenide thin film layers.
- Fabrication of Zinc sulfide-selenide/Nickel oxide heterojunction devices.
- Rectifying behavior and 500 mV open circuit voltage achieved.

1. Introduction

In the global energy market photovoltaics (PV) is taking an ever-growing share of the production capacity [1]. Every year hundred new gigawatt peak of solar power is installed worldwide, with the largest part of the market being covered by Si solar modules that can be installed in fields or can be added on rooftops of buildings [2]. To integrate the photovoltaic systems into a house more aesthetically, building-integrated solar solutions are searched for [3,4]. One possibility of adding photovoltaics into a building, without changing the overall appearance of the building, would be to integrate the photovoltaic cells in the windows. Especially office buildings typically have a very large window area, which could offer an interesting opportunity for integrating photovoltaics, if only the cells could be made at least partly transparent to visible light. Several solutions to this problem are already being researched or commercialized [5-12]. The European project Tech4Win is targeting this challenge by using a technology that is based on a tandem photovoltaic cell consisting of a UV absorbing cell on top of an organic photovoltaic cell that is only absorbing the IR light [13]. In this contribution we report on the development of a possible solution for the top cell, which is only absorbing the UV irradiation of the solar spectrum, letting the visible and IR portion go through as unhindered as possible. At first, we develop an absorber layer with a band gap of about 3 eV, which will absorb the UV light, but let the visible light pass through. The material of choice in this contribution is a mixture of ZnS and ZnSe, Zn(S,Se). ZnSe and ZnS in fact are chalcogenide materials with a large band gap of 3.6 and 2.6 eV respectively [14,15]. Therefore, the mixed material Zn(S,Se) will allow a band gap with a value between 2.6 and 3.6 eV and eventually even some band gap grading, depending on the relative Se/S content. Other solutions that will allow a similar device functionality, only absorbing the UV part of the solar spectrum, rely for example on ZnO or Zn(O,S) absorbers [6,16]. ZnS and ZnSe based materials are already in use for solar applications, mainly being studied as buffer layer materials [17-20]. In the present contribution we investigate their use also as absorber materials for solar cells.

In the next section we explain the experimental methods used to fabricate the absorber layer. Then, in section 3, we present a study on the fabrication method we have used: metal deposition followed by selenization and/or sulfurization in H_2Se or H_2S. We will describe how we can prevent the formation of holes in the thin film layer during the crystallization process. In section 4 we will present a doping study, where we have added extrinsic doping elements to the absorber to increase its conductivity. Finally in section 5, we will describe the photovoltaic devices that we have fabricated based on a Zn(S,Se) absorber, a NiO buffer layer and two transparent electrodes.

2. Experimental details

We have fabricated ZnS, ZnSe and mixed Zn(S,Se) layers using a two-step process, which is schematically shown in Fig. 1. First, we have deposited a thin layer of Zn using electron beam evaporation in a Pfeiffer PLS 580 evaporation chamber on a commercial soda-lime glass or Fluorine doped Tin Oxide (FTO) substrate with 10 Ohm square sheet resistance. For our doping experiments, we first deposited a thin layer of the doping element, typically 0.3 nm, followed by the Zn layer. Different thicknesses of Zn layers were tried, ranging from 100 nm to 300 nm. The thickness of the different layers was measured with a quartz microbalance. Then the Zn layer was annealed at temperatures around 500°C in an Annealsys AS-150 rapid thermal anneal chamber in the presence of 100 % H_2S for ZnS formation, 10 % H_2Se in N_2 for ZnSe formation or a mixture of both H_2S and H_2Se for the mixed Zn(S,Se) layers. The anneal conditions had to be optimized in order to reach pinhole-free thin film layers of ZnS, ZnSe and Zn(S,Se) and the details for the process conditions used to fabricate the pinhole-free layers will be discussed in the next section.

3. Optimizing the properties of ZnS, ZnSe and Zn(S,Se) thin film layers

Our baseline process for the fabrication of chalcogenide thin film layers consists of an anneal of 15 minutes in an atmosphere of H_2Se and/or H_2S at elevated temperatures. Because H_2Se is more reactive

than H_2S, the temperatures we use are 450˚C for H_2Se anneals and 520˚C for H_2S anneals. To fabricate samples with a 50/50 ratio of S and Se, we introduce a 100 times higher partial pressure of H_2S as compared to H_2Se into the chamber. Figure 2 shows the three baseline samples that we have fabricated on glass substrates using a 300 nm thick Zn starting layer: ZnS, ZnSe and mixed Zn(S,Se) respectively. After the selenization/sulfurization process, the final layer thickness is about 1 μm. It can be observed that the ZnSe has a yellow color, the ZnS has a neutral color, whereas the Zn(S,Se) sample has a very slight yellowish color. Figure 3 shows the measurement of the transmittance data of the three different samples and the Tauc plots of the layers. The band gaps that can be derived from the Tauc plots of this data are 3.6, 3.0 and 2.6 eV for the ZnS, Zn(S,Se) and ZnSe layers respectively, whereas the average visible transmittances of the layers are 60 %, 55 % and 36 % respectively. The average visible transmittance of the device was calculated from the transmittance in the optical range, by integrating it over the photoptic response of the human eye. A definition of the average visible transmittance is given in [21]. One of the main functions of the UV-based absorber layer is to act as a UV filter and to absorb all the UV light with wavelengths smaller than 400 nm to protect the underlying layers of the tandem solar cell structure from the degrading UV light. In figure 3 it can be seen that both the Zn(S,Se) and the ZnSe layers do fulfil this requirement. Due to its high bandgap, ZnS does not absorb all the UV light and was therefore disregarded as a possible absorber layer. Because the average visible transmittance of the Zn(S,Se) layer is considerably higher, and the nuisance of the yellow color for a potential window application is lower, Zn(S,Se) was preferred over ZnSe as an absorber layer for this transparent PV application. In the following, we will therefore focus on the optimization of the anneal conditions that lead to the highest quality Zn(S,Se) layers.

Figure 4 shows a top view scanning electron microscopy (SEM) image of a 300 nm thick Zn(S,Se) layer and a 1 μm thick Zn(S,Se) layer fabricated with our standard baseline process. This baseline process consists of a 15 minute 520˚C anneal in the presence of H_2Se and H_2S in a 1/100 partial pressure ratio.

In fact, the H_2Se partial pressure is 200 Pa and the H_2S partial pressure for the baseline process is 20 kPa. The total pressure is brought up to 50 kPa using N_2. This anneal leads to a 50/50 ratio between Sulfur and Selenium in the final absorber, as measured by energy-dispersive X-ray spectroscopy. As becomes visible in the image, the 1 µm thick sample has occasional pinholes in the absorber layer, whereas the thinner 300 nm thick sample has many of these pinholes. For thin film electronic device, such as solar cells, every such pinhole represents a possible shunting channel, degrading the device performance. Therefore, an optimization of the selenization/sulfurization parameters had to be performed to reduce the number of pinholes. It seems quite likely that the pinholes in the layer are due to the high partial pressure of Zn at the reaction temperatures. The vapor pressure of Zn at 500°C is about 100 Pa [23], so the upward pressure on a thin layer of Zn(S,Se) that has just crystallized on top of a layer of Zn can be quite substantial. Therefore, the rationale behind our optimization trials was to roughen up the Zn layer as much as possible, in order to avoid a closed layer of Zn(S,Se) in the early stages of the crystallization. We have therefore developed a process which consisted of a 10 minute pre-anneal of the Zn layer in N_2 at 250°C, followed by the introduction of the reaction gases and a very fast ramp of the temperature to 520°C at about 10°C/s. This lead to a layer of Zn(S,Se) without pinholes in the case of the 1 µm thick absorber layer and a reduction in the amount of pinholes for the thinner 300 nm thick Zn(S,Se) layer. Figure 5 shows a SEM micrograph of the optimized 1µm thick ZnSe, Zn(S,Se) and ZnS layers. A full reduction of the number of pinholes for the thinner 300 nm thick layer could so far not be obtained with our process. The device experiments that are presented in section 5 have therefore been performed with 1 µm thick absorber layers, even though a somewhat thinner layer thickness would have been optimal from a transparency point of view.

4. Doping the Zn(S,Se) layer

Measuring the sheet resistance of the 1 μm thick Zn(S,Se) layer, using two contact pads made of silver paste, revealed a very high resistivity value of 1 MΩ cm. To reduce the resistivity of the Zn(S,Se) layer we have added different possible doping elements to the stack. To add the doping elements to the absorber we have chosen to evaporate a 0.3 nm layer of the doping material before the deposition of the Zn layer. The total stack was then processed in the anneal oven, to get an intermixing of the doping elements with the Zn layer during the selenization/sulfurization process. We have tried different layers: LiF, Al, Ge, MgF_2, Cu and Sn. Whereas the LiF did not lead to a reduction of the layer resistivity, the addition of the other elements did reduce the resistivity of the Zn(S,Se) layer. ZnS and ZnSe are intrinsically n-type materials, due to the action of both interstitial Zn or S vacancies [22]. Al, Ge and Sn are known n-type dopants in ZnS or ZnSe, whereas Cu_{Zn} antisite dopant is known to be p-type after a high temperature activation anneal [22]. In the present fabrication procedure, we did not do a high temperature activation anneal and the Cu is likely to add to the n-type doping as an interstitial atom in the Zn(S,Se) lattice. Resistivities measured after addition of the doping materials were 30, 10, 10, 15 and 13 kΩ cm for Al, Ge, MgF_2, Cu and Sn respectively. Even though from a resistivity point of view the five different doping materials were quite equivalent, we have chosen the Cu doping, because it was the only element that did not lead to a milky appearance of the Zn(S,Se) layer, but left the transparency of the layer untouched.

5. Zn(S,Se) solar cell devices

Following the optimization of the absorber layer, we also fabricated solar cell devices. We have combined the n-type Zn(S,Se) absorber layer with another transparent oxide material, namely p-type NiO. As a back contact material, we have used a commercial FTO layer on a glass substrate. Unfortunately, the FTO also reacted with the Se during the selenization process of the Zn(S,Se), such that we had to use a protective layer between the FTO and the Zn(S,Se). We have found that a 200 nm

layer of Indium Zinc Oxide (IZO) works quite well for protecting the FTO layer. This layer was deposited by sputtering on top of the commercial FTO/glass substrate. A slight reduction of the transparency can be observed using that protection layer, as can be seen from the transmittance measurement of the stack including the back contact on Figure 6. Due to higher absorption in the blue wavelength region, the yellowish appearance of the stack on the back contact becomes stronger, as becomes visible from the photograph in Figure 6.

The device was finished by the deposition of a 50 nm NiO layer deposited by reactive sputtering from a Ni target in an Oxygen plasma. The top contact was a 10 nm thick semi-transparent Ag layer that was evaporated through a shadow mask, such that the final stack layout is: Glass/FTO/IZO/Zn(S,Se):Cu/NiO/Ag. The area of the Ag top contact was 1 mm^2, defining the active area of the device. Figure 7 shows the current density of the finished device as a function of voltage measured in the dark on a logarithmic scale and on a linear scale. A very decent rectifying behaviour can be observed. In the dark the device shows a shunt resistance of about 175 kΩ cm^2 and a series resistance of about 3 Ω cm^2. The diode properties could roughly be determined as well with a reverse saturation current J_0 of about 3 10^{-20} A/cm^2 and an ideality factor of about 1.4. Biasing beyond voltages of 1 V lead to strong hysteresis effects though, which disappeared again after a few hours of waiting or after a soft anneal at 150°C, such that it is likely that deep defects are present in the Zn(S,Se) absorber layer. Also shown in Figure 7 is the current density as a function of voltage under AM1.5G illumination. The device operates as a weak solar cell and shows a very small short circuit current of about 100 µA/cm^2, an open circuit voltage of about 550 mV, a shunt resistance of 75 kΩ cm^2, a series resistance of 1.6 Ω cm^2 and a fill factor of about 65 %. The power conversion efficiency is about 0.05%. The low power conversion efficiency is likely limited by the same defects that lead to the hysteresis behavior in the J-V curves, as these are deep defect states with long time constants and are therefore also strong recombination centers for minority carriers.

5. Conclusions

We have fabricated thin Zn(S,Se) thin film layers on transparent back contact substrates for semi-transparent UV-sensitive photovoltaic applications. The developed layers are about 1 µm thick and contain roughly the same amount of S and Se. This composition was chosen to have a band gap of the material of 3 eV. Such a band gap of 3 eV allows for the material to be very transparent to visible light, whereas it absorbs the integrity of the UV light, therefore also acts as a UV filter. A process based on an anneal at high temperature in a H_2Se and H_2S containing atmosphere was optimized in order to fabricate continuous Zn(S,Se) absorber layers. The layers were doped with different elements, which increased the conductivity of the layers by three orders of magnitude as compared to the intrinsic Zn(S,Se) case. Finally, devices were fabricated with the following stack layout: Glass/FTO/IZO/Zn(S,Se):Cu/NiO/Ag. These devices showed a small photocurrent of about 100 µA/cm^2 and a 550 mV open circuit voltage under AM1.5G illumination, which corresponds to a 0.05 % power conversion efficiency. This low power conversion efficiency is likely due to deep defect states in the devices, which also leads to strong hysteresis in the J-V curves.

Acknowledgments

This work has received funding from the European Union H2020 Framework Program under Grant Agreement no. 826002 (Tech4Win).

References

[1] P. R. Wolfe, The Solar Generation: Childhood and Adolescence of Terrestrial Photovoltaics, ISBN: 978-1-119-42558-8, Wiley-IEEE Press (2018).

[2] M. A. Green, Commercial progress and challenges for photovoltaics, Nat. Energy 1 (2016) 15015. https://doi.org/10.1038/nenergy.2015.15.

[3] R. P. N. P. Weerasinghe, R. J. Yang, R. Wakefield, E. Too, T. Le, R. Corkish. S. Chen, and C. Wang, Economic viability of building integrated photovoltaics: A review of forty-five (45) non-domestic buildings in twelve (12) western countries, Renewable & sustainable energy reviews 137 (2021) 110622 1-19. https://doi.org/10.1016/j.rser.2020.110622.

[4] B. P. Jelle, C. Breivik and H. D. Røkenes, Building integrated photovoltaic products: a state-of-the-art review and future research opportunities, Sol. Energy Mater. Sol. Cells 100 (2012) 69–96. https://doi.org/10.1016/j.solmat.2011.12.016.

[5] J. Sun and J. J. Jasieniak, Semi-transparent solar cells, J. Phys. D: Appl. Phys. 50 (2017) 093001 1-28. https://doi.org/10.1088/1361-6463/aa53d7.

[6] A. J. Lopez-Garcia, A. Bauer, R. Fonoll Rubio, D. Payno, Z. Jehl Li-Kao, S. Kazim, D. Hariskos, V. Izquierdo-Roca, E. Saucedo, A. Pérez-Rodríguez, UV-Selective Optically Transparent Zn(O,S)-Based Solar Cells, Sol. RRL 4 Issue 11 (2020), 2000470 1-7. https://doi.org/10.1002/solr.202000470.

[7] L. J. Wook, M. Shin, D. J. Lee, L. S. Hyun and Y.S. Jin, Highly transparent amorphous silicon solar cells fabricated using thin absorber and high-bandgap energy n/i-interface layers, Sol. Energy Mater. Sol. Cells 128 (2014) 301–306. https://doi.org/10.1016/j.solmat.2014.05.041.

[8] M.Saifullah, S.J. Ahn, J. Gwak, S. Ahn, K. Kim, J. Cho, J. H. Park, Y. J. Eo, A. Cho, J.-S. Yoo and J. H. Yun, Development of Semitransparent CIGS thin-film solar cells modified with a sulfurized-AgGa layer for building applications, J. Mater. Chem. A 4 (2016) 10542–10551. https://doi.org/10.1039/C6TA01909A.

[9] V. V. Plotnikov, C. W. Carter, J. M. Stayancho, N. R. Paudel, H. Mahabaduge, D. Kwon, C. R. Grice and A. D. Compaan, Semitransparent PV windows with sputtered CdS/CdTe thin films, Proceedings of the 39th IEEE Photovoltaic Specialists Conf. (PVSC), Tampa, Florida (2013) 405–408. https://doi.org/10.1109/PVSC.2013.6744178.

[10] D. Joly, L. Pelleja, S. Narbey, F. Oswald, T. Meyer, Y. Kervella, P. Maldivi, J. N. Clifford, E. Palomares and R. Demadrille, Metal-free organic sensitizers with narrow absorption in the visible for solar cells exceeding 10% efficiency, Energy Environ. Sci. 8 (2015) 2010–2018. https://doi.org/10.1039/C5EE00444F.

[11] F. Guo, H. Azimi, Y. Hou, T. Przybilla, M. Hu, C. Bronnbauer, S. Langner, E. Spiecker, K. Forberich and C.J. Brabec, High-performance semitransparent perovskite solar cells with solution-processed silver nanowires as top electrodes, Nanoscale 7 (2014) 1642–1649. https://doi.org/10.1039/C4NR06033D.

[12] X. Ren, X. Li and W. C. H. Choy, Optically enhanced semi-transparent organic solar cells through hybrid metal/nanoparticle/dielectric nanostructure, Nano Energy 17 (2015) 187–195. https://doi.org/10.1016/j.nanoen.2015.08.014.

[13] www.tech4win.eu, European Union H2020 Framework Program under Grant Agreement no. 826002.

[14] M. A. Avilés, J. M. Córdoba, M. J. Sayagués, and F. J. Gotor, Tailoring the Band Gap in the ZnS/ZnSe System: Solid Solutions by a Mechanically Induced Self-Sustaining Reaction, Inorg. Chem. 58 Issue 4 (2019) 2565–2575. https://doi.org/10.1021/acs.inorgchem.8b03183.

[15] R. Woods-Robinson, Y. Han, H. Zhang, T. Ablekim, I. Khan, K. A. Persson, and A. Zakutayev, Wide Band Gap Chalcogenide Semiconductors, Chem. Rev. 120 (2020) 4007−4055. https://doi.org/10.1021/acs.chemrev.9b00600.

[16] S. Kim, M. Patelab, T. T. Nguyen, J.Yi, Ching-PingWong and J. Kim, Si-embedded metal oxide transparent solar cells, Nano Energy 77 (2020) 105090 1-9. https://doi.org/10.1016/j.nanoen.2020.105090.

[17] Kaushalya, S. L. Patel, A. Purohit, S. Chander, S, M.S. Dhaka, Thermal annealing evolution to physical properties of ZnS thin films as buffer layer for solar cell applications, Physica E: Low-

dimensional Systems and Nanostructures 101 (2018) 174-177. https://doi.org/10.1016/j.physe.2018.04.006.

[18] D. Agrawal, S.L. Patel, Himanshu, S. Chander, M.D. Kannan, M.S. Dhaka, Role of low-cost non-toxic $MgCl_2$ treatment on ZnS films: Optimization of physical properties for buffer layers, Optik 199. (2019) 163307 1-6. https://doi.org/10.1016/j.ijleo.2019.163307.

[19] S. Chuhadiya, R. Sharma, Himanshu, S.L. Patel, S. Chander, M.D. Kannan, M.S. Dhaka, Thermal annealing induced physical properties of ZnSe thin films for buffer layer in solar cells, Physica E: Low-dimensional Systems and Nanostructures 117 (2020), 113845. https://doi.org/10.1016/j.physe.2019.113845.

[20] D. Agrawal, S.L. Patel, Himanshu, S. Chander, M.S. Dhaka, Impact of Hydrogen flow rate on physical properties of ZnS thin films: As potential buffer layer in solar cells, Optical Materials 105 (2020) 109899 1-7. https://doi.org/10.1016/j.optmat.2020.109899.

[21] Chenchen Yang, Dianyi Liu, Matthew Bates, Miles C. Barr, Richard R. Lunt, How to Accurately Report Transparent Solar Cells, Joule 3 (2019) 1795–1809. https://doi.org/10.1016/j.joule.2019.06.005.

[22] R. Woods-Robinson, Y. Han, H. Zhang, T. Ablekim, I. Khan, K. A. Persson, and A. Zakutayev, Wide Band Gap Chalcogenide Semiconductors, Chem. Rev. 120 (2020), 4007−4055. https://dx.doi.org/10.1021/acs.chemrev.9b00600.

[23] J. D. McKinley Jr. and J. E. Vance, The Vapor Pressure of Zinc between 150° and 350°C, J. Chem. Phys. 22, (1954) 1120-1124. https://doi.org/10.1063/1.1740276.

Figures and figure captions

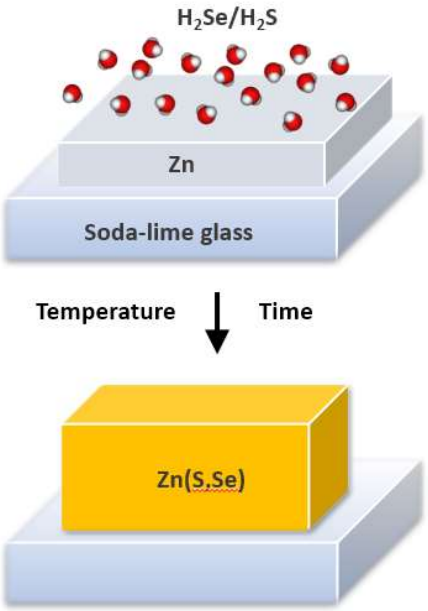

Figure 1: *Schematic representation of the fabrication process of the thin film Zn(S,Se) layers.*

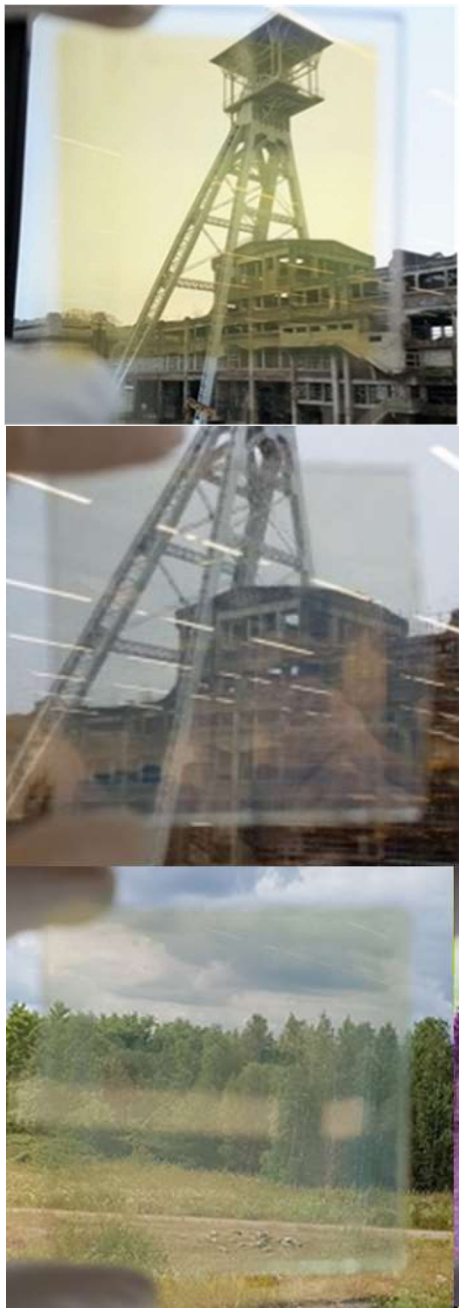

Figure 2: *Photographs of a 1 μm thick ZnSe (top), ZnS (middle) and Zn(S,Se) (bottom) layer on a glass substrate.*

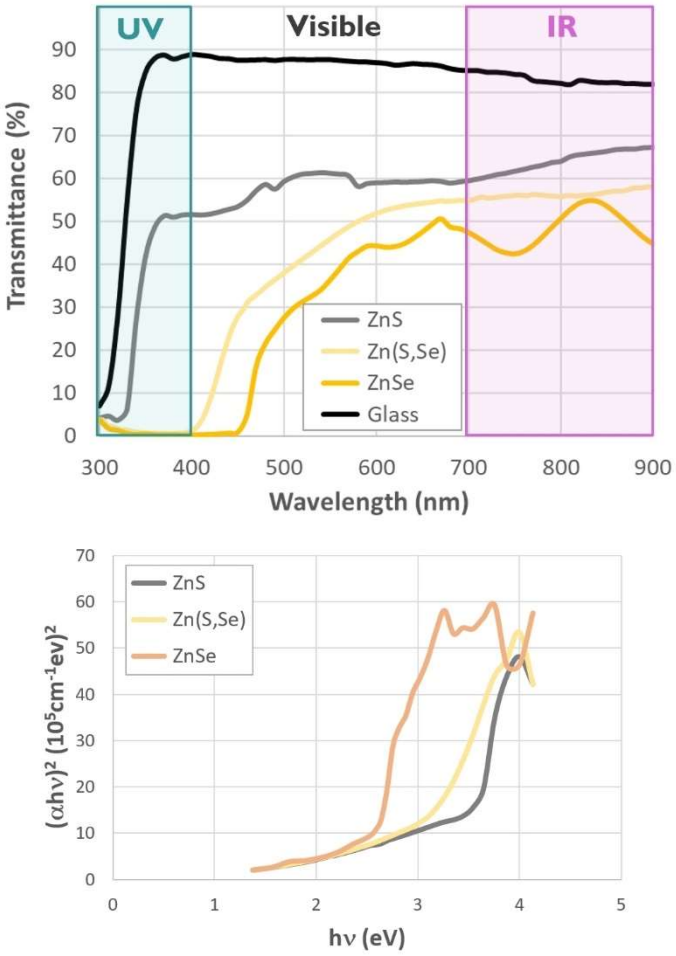

Figure 3: *Transmittance as a function of wavelength for the 1 µm ZnSe, ZnS and Zn(S,Se) layers on a glass substrate. As a comparison the transmittance of the 3 mm thick glass substrate is shown as well (top). Tauc plots of the 1 µm ZnSe, ZnS and Zn(S,Se) layers on a glass substrate (bottom).*

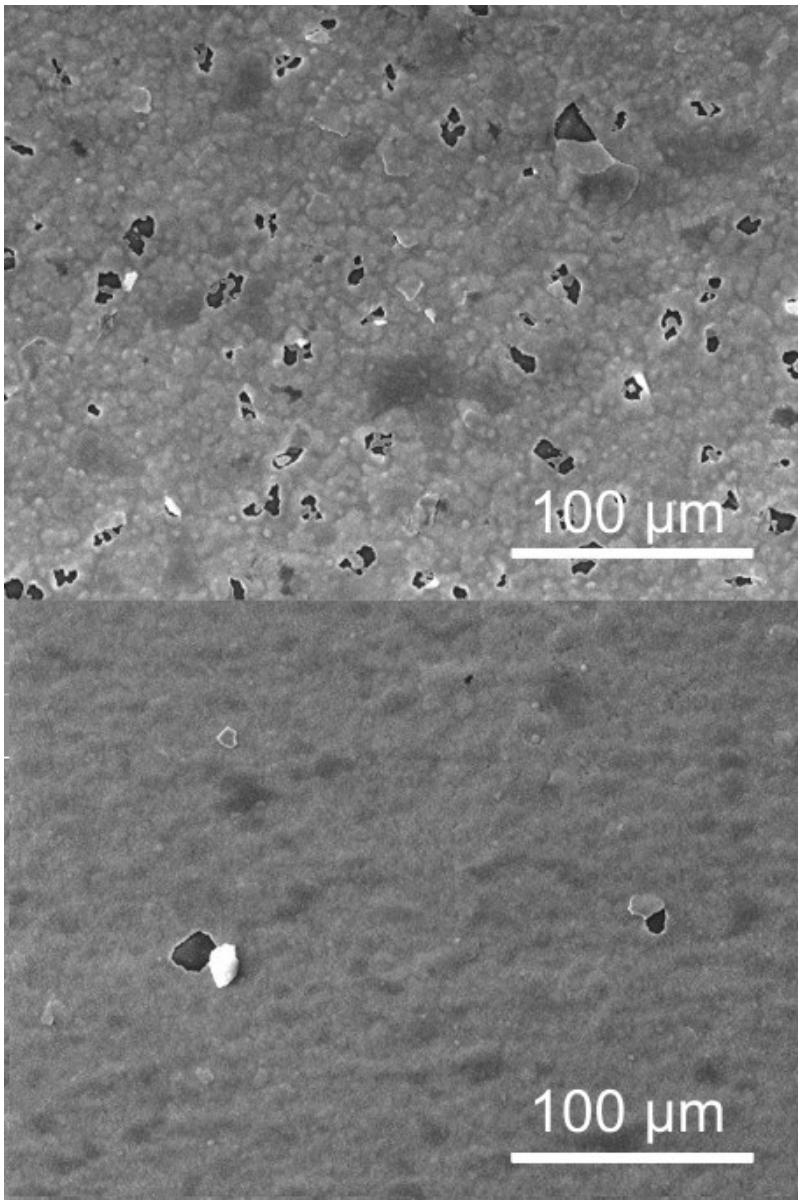

Figure 4: *Top view SEM images of a 300 nm (top) and 1 µm (bottom) thick Zn(S,Se) layer on a glass substrate before process optimization with holes visible in the film layer.*

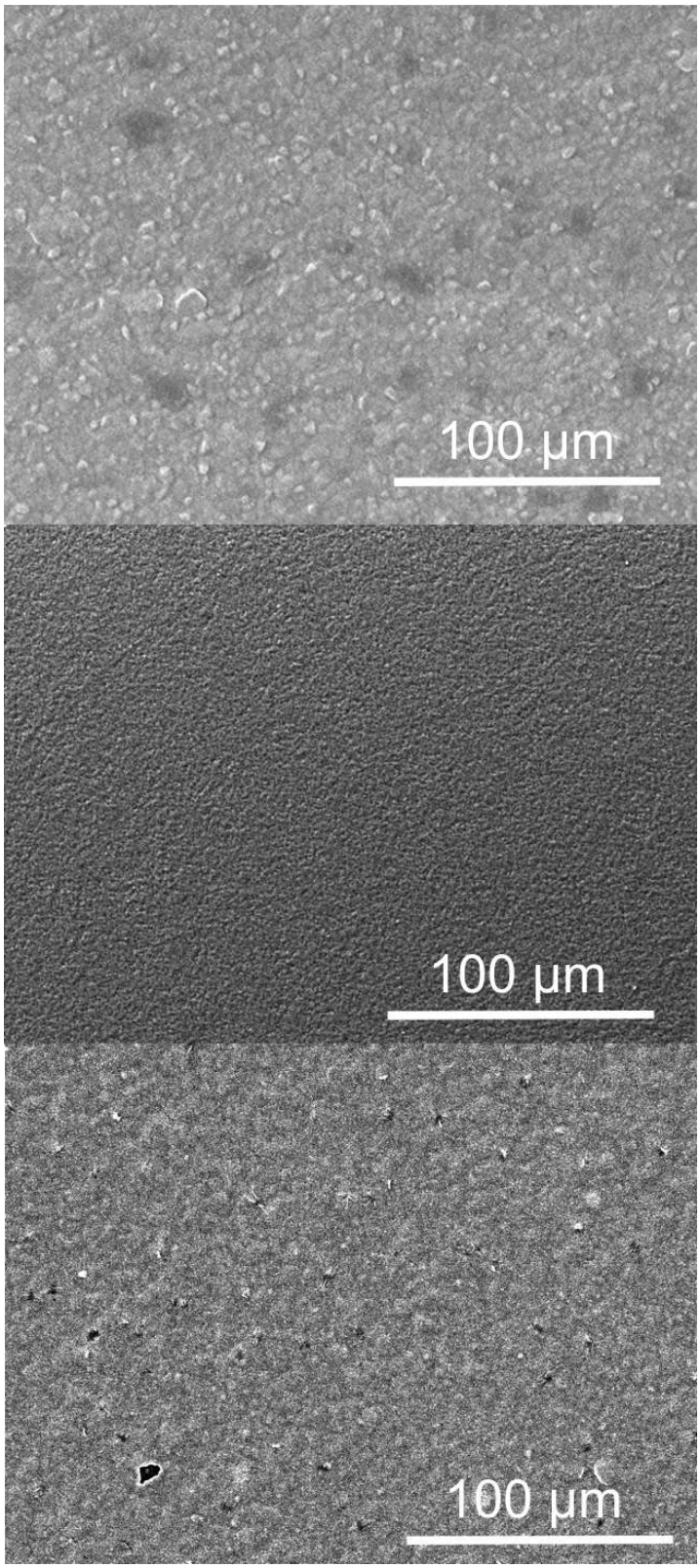

Figure 5: *Top-view SEM image of a 1 µm thick ZnSe (top), Zn(S,Se) (middle) and ZnS (bottom) layer on a glass substrate after process optimization.*

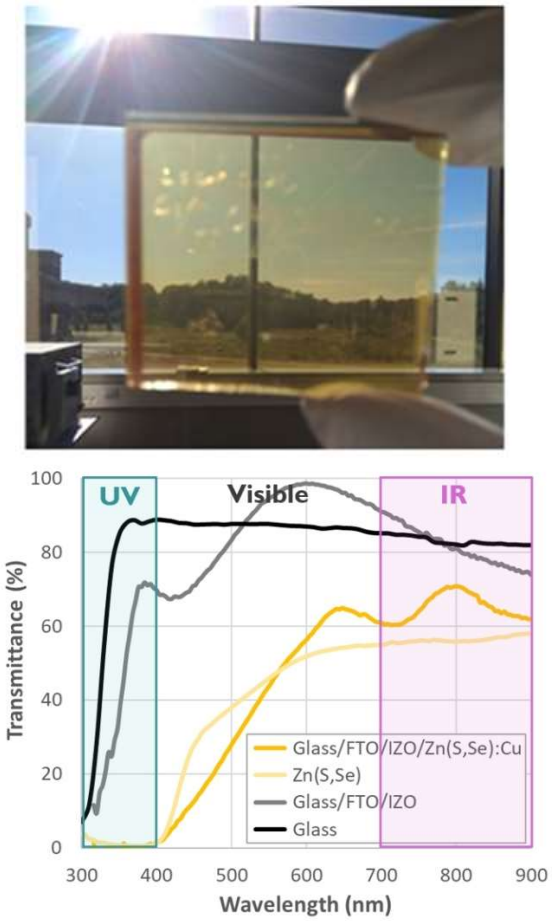

Figure 6: *Photograph of a 1 µm thick Cu-doped Zn(S,Se) layer on a glass/FTO/IZO substrate (top). Transmittance of the 1 µm thick Cu-doped Zn(S,Se) layer on a glass/FTO/IZO substrate (bottom).*

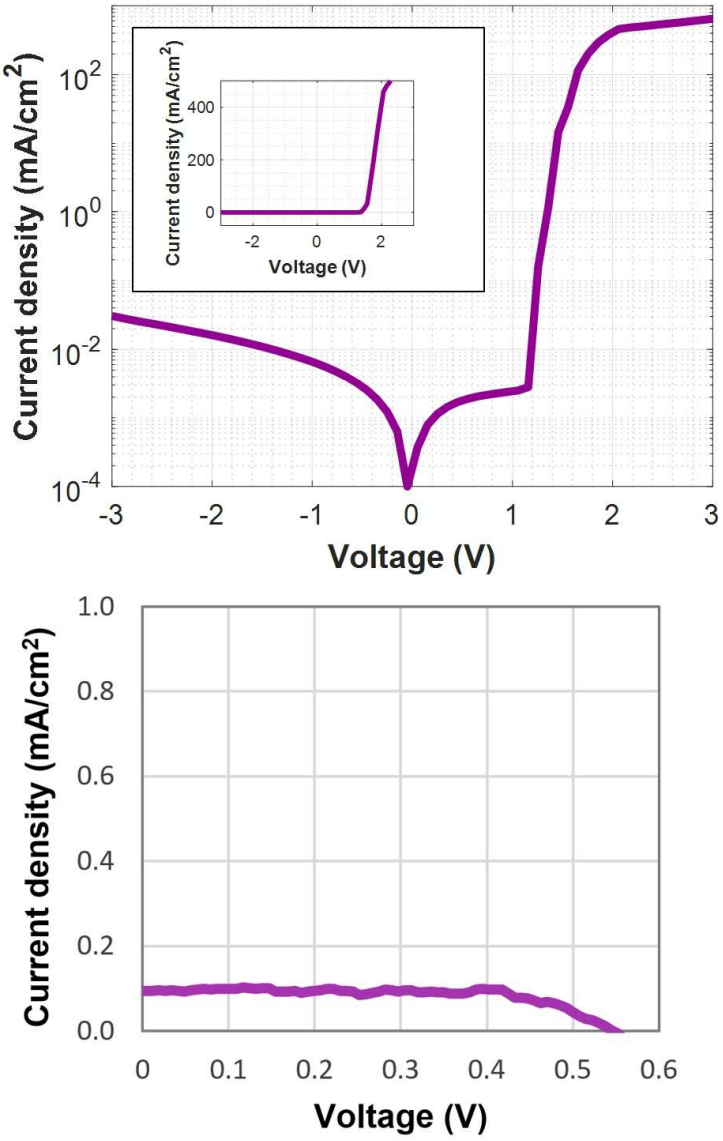

Figure 7: *Current density versus bias voltage for the Zn(S,Se) device in the dark. The inset shows the same data on a linear y-scale (top). Current density versus bias voltage for the Zn(S,Se) device under AM1.5G illumination (bottom).*